JVI Journals.ASM.org

Tropism and Infectivity of Influenza Virus, Including Highly Pathogenic Avian H5N1 Virus, in Ferret Tracheal Differentiated Primary Epithelial Cell Cultures

Hui Zeng,[a] Cynthia S. Goldsmith,[b] Taronna R. Maines,[a] Jessica A. Belser,[a] Kortney M. Gustin,[a] Andrew Pekosz,[c] Sherif R. Zaki,[b] Jacqueline M. Katz,[a] Terrence M. Tumpey[a]

Immunology and Pathogenesis Branch, Influenza Division, National Center for Immunization and Respiratory Disease,[a] and Infectious Disease Pathology Branch, Division of High Consequence Pathogens and Pathology, National Center for Emerging and Zoonotic Infectious Diseases,[b] Centers for Disease Control and Prevention, Atlanta, Georgia, USA; W. Harry Feinstone Department of Molecular Microbiology and Immunology, The Johns Hopkins Bloomberg School of Public Health, Baltimore, Maryland, USA[c]

Tropism and adaptation of influenza viruses to new hosts is partly dependent on the distribution of the sialic acid (SA) receptors to which the viral hemagglutinin (HA) binds. Ferrets have been established as a valuable *in vivo* model of influenza virus pathogenesis and transmission because of similarities to humans in the distribution of HA receptors and in clinical signs of infection. In this study, we developed a ferret tracheal differentiated primary epithelial cell culture model that consisted of a layered epithelium structure with ciliated and nonciliated cells on its apical surface. We found that human-like (α2,6-linked) receptors predominated on ciliated cells, whereas avian-like (α2,3-linked) receptors, which were less abundant, were presented on nonciliated cells. When we compared the tropism and infectivity of three human (H1 and H3) and two avian (H1 and H5) influenza viruses, we observed that the human influenza viruses primarily infected ciliated cells and replicated efficiently, whereas a highly pathogenic avian H5N1 virus (A/Vietnam/1203/2004) replicated efficiently within nonciliated cells despite a low initial infection rate. Furthermore, compared to other influenza viruses tested, VN/1203 virus replicated more efficiently in cells isolated from the lower trachea and at a higher temperature (37°C) compared to a lower temperature (33°C). VN/1203 virus infection also induced higher levels of immune mediator genes and cell death, and virus was recovered from the basolateral side of the cell monolayer. This ferret tracheal differentiated primary epithelial cell culture system provides a valuable *in vitro* model for studying cellular tropism, infectivity, and the pathogenesis of influenza viruses.

Influenza A viruses pose a significant threat to public health. Human influenza viruses target cells of the upper respiratory tract, resulting in clinical symptoms such as fever, cough, headache, and malaise (1, 2). In the past 2 decades, influenza viruses of avian origin, including novel H5, H7, and H9 subtypes, have infected humans as a result of transmission from avian species. In particular, human infections with highly pathogenic avian influenza (HPAI) H5N1 viruses often results in severe clinical illness, including pneumonia with impairment of gas exchange, and have been associated with high viral loads and exacerbated cytokine production in the lower respiratory tract (3, 4).

In the first step of influenza virus infection, the hemagglutinin (HA) protein binds to sialic acid (SA) residues present on the surface of host cells. Human influenza viruses preferentially bind to α2,6-linked SA, whereas avian influenza viruses bind to α2,3-linked SA. Cellular tropism and the infectivity of influenza viruses are primarily determined by the distribution of these two SA receptors in the human respiratory tract. Lectin histochemistry studies of human airway tissues have indicated that both forms of SA can be found throughout the respiratory tract. α2,6-linked SA receptors are found at higher levels on epithelial cells, including ciliated cells and, to a lesser extent, on goblet cells in the upper respiratory tract (5–7). Conversely, α2,3-linked SA receptors are found at higher levels on nonciliated bronchiolar cells and alveolar type II cells in the lower respiratory tract (2, 5, 6, 8). Consistent with these findings, studies of virus attachment have shown that human influenza viruses bound more abundantly to the upper respiratory tract than avian influenza viruses (2, 9, 10). Human influenza viruses attach primarily to ciliated epithelial cells and to a lesser extent to goblet cells in the upper respiratory tract, as well as to type I pneumocytes in the alveoli (6, 10, 11). In contrast, avian influenza viruses generally attach to type II pneumocytes, alveolar macrophages, and nonciliated epithelial cells in the terminal bronchioles and alveoli in the lower respiratory tract (11–14). Ferrets have been used extensively to evaluate influenza virus pathogenicity and transmissibility (15–17). The recognition of the ferret's natural susceptibility to influenza virus infection and similarities to humans in lung physiology, airway morphology, and cell types present in the respiratory tract make it an ideal animal model for studying influenza viruses (11, 18–20). Clinical signs of illness are similar in ferrets and humans, likely in part because the distribution of α2,6- and α2,3-linked SA receptors in the ferret respiratory tract resembles that observed in humans (11, 19). Recently, it has been shown that α2,6-linked SA receptors are more abundant than α2,3-linked receptors throughout the ferret respiratory tract (21, 22). Moreover, virus attachment studies have shown similarities between the ferret and human respiratory tract, where human influenza viruses attached more abundantly to cil-

Received 15 October 2012 **Accepted** 10 December 2012
Published ahead of print 19 December 2012
Address correspondence to Terrence M. Tumpey, tft9@cdc.gov.

doi:10.1128/JVI.02885-12

iated cells and to a lesser extent to goblet cells in the upper respiratory tract as well as type I pneumocytes. Conversely, labeled avian influenza viruses attach to nonciliated epithelial cells and type II pneumocytes in the lower respiratory tract (11, 23). However, data suggest that the ferret trachea has less abundant goblet cells and moderate differences in receptor distribution in airways compared to the human airway (21, 23).

Culture systems of differentiated primary epithelial cells from human and animal airways, especially derived from the trachea, provide valuable *in vitro* models for characterization of cellular tropism and infectivity of influenza viruses (24–31). Differentiated tracheal epithelial cell cultures offer numerous advantages, including greater control of experimental conditions and the ability to study epithelial cell function in the absence of other cell types, such as cells representing submucosal glands, all of which can contribute valuable information for *in vivo* studies. The tracheal epithelium is pseudostratified and columnar, consisting of ciliated cells that propel mucus and secretory cells (including goblet cells) on the surface and basal cells that are not in contact with the airway lumen (32). Airway epithelial cells from ferret tracheas have been successfully grown and polarized *in vitro* for comparison of its electrophysiologic properties (33); however, such cells have not been used to characterize influenza virus-host interactions at the cellular and molecular levels. In the present study, we developed and characterized cultures of ferret tracheal differentiated primary epithelial cell (FTE) and used this model to study cellular tropism and infectivity of both human and avian influenza viruses. We found that human viruses mainly infected ciliated cells with α2,6-linked SA receptors, whereas avian influenza viruses mainly infected nonciliated cells. The human influenza viruses and the HPAI H5N1 virus studied replicated efficiently in FTE cells; however, only infectious H5N1 virus was recovered from the basolateral side of the cell monolayer. Furthermore, HPAI H5N1 virus infection resulted in a higher level of cell death and the induction of higher levels of proinflammatory mediators compared to the other influenza viruses studied.

MATERIALS AND METHODS

Viruses. An HPAI H5N1 subtype virus, A/Vietnam/1204/2003 (VN/1203), was grown in the allantoic cavities of 10-day-old embryonated hen's eggs for 24 to 26 h at 37°C. The H3N2 virus A/Wisconsin/67/2005 (Wisconsin/67) was grown in eggs for 48 h at 33.5°C. Allantoic fluid was clarified by centrifugation, aliquoted, and stored at −70°C. The seasonal H1N1 virus A/Brisbane/59/2007 (Brisbane/59), the 2009 pandemic H1N1 virus A/Mexico/4482/2009 (Mexico/4482), and the low-pathogenicity avian H1N1 virus A/Duck/New York/15024/96 (Dk/NY) were propagated in MDCK cells at 37°C for 48 h. The supernatants were clarified by centrifugation, aliquoted, and stored at −70°C. Virus titers were determined by plaque assay. The identity of virus genes was confirmed by sequence analysis to verify that no inadvertent mutations were present during the generation of virus stocks. All research with HPAI H5 subtype viruses was conducted under biosafety level 3 containment, including enhancements required by the U.S. Department of Agriculture and the National Select Agent Program (34–36).

Ferret tracheal epithelial (FTE) cells isolation and culture. Male Fitch ferrets, 8 to 18 months of age (Triple F Farms, Sayre, PA), were anesthetized with an intramuscular injection of a ketamine-atropine-xylazine cocktail and euthanized for necropsy. Ferret tracheas were excised from below the larynx to the major bronchi and submerged in cold modified Eagle medium (MEM) and processed individually. The tracheas were further cleaned in cold Mg^{2+} and Ca^{2+} free phosphate-buffered saline (PBS) to remove extraneous attached tissue. Tracheas were then sliced longitudinally and digested in MEM containing 1.4 mg of pronase/ml and 0.1 mg of DNase I/ml (Roche, Indianapolis, IN) for 18 to 36 h and then 10% fetal bovine serum (FBS; without heat inactivation) was added to stop the protease reaction. Each resulting cell suspension was moved to a new tube and centrifuged at 200 × *g* for 10 min at 4°C. The cell pellet from each trachea was suspended in tracheal epithelial cell (TEC) Basic medium (Dulbecco modified Eagle medium nutrient mixture F12 [1:1] containing 25 mM HEPES, 100 U/ml of penicillin, 100 μg/ml of streptomycin, and 1× nonessential amino acids) with 5% FBS (without heat inactivation). The cells were transferred to a tissue culture dish, followed by incubation for 3 h at 37°C to remove contaminating fibroblasts.

The epithelial cells isolated from individual ferrets were suspended in TEC Plus medium, which contained TEC Basic medium supplemented with a BEGM SingleQuot kit (Lonza, Walkersville, MD), and 15 ng of retinoic acid/ml. The cells were plated on collagen-coated, 0.4-μm-pore-size membranes on 12- and 24-well transwell inserts (Corning Costar, Corning, NY) at a concentration of 2.5×10^5 to 5×10^5 cells/cm^2 and grown as liquid covered culture for 2 to 3 days with apical and basolateral media changed each day to reach a confluent monolayer. After reaching a transepithelial resistance of >1,000 Ω·cm^2, the apical medium was removed to create an air-liquid interface (ALI), and basolateral media were changed every 1 to 2 days for 3 to 4 weeks.

For the experiments evaluating different portions (upper and lower) of the ferret trachea, whole tracheas acquired from three individual animals were removed aseptically. The trachea tissues were laid flat and divided equally by a cut made in the middle. The upper and lower trachea portions were processed separately according to the methods described above. Cells were seeded onto transwell membranes and cultured for 3 to 4 weeks before use.

Influenza A virus infections. FTE cells cultured in an ALI were washed three times with TEC Plus medium for 10 min to remove mucus and were infected apically with influenza virus at the indicated multiplicity of infection (MOI). After 1 h of incubation, the inocula were removed, and the cells were washed three times to remove unattached virus. FTE cells remained in ALI, and the basolateral media were changed daily for the duration of each experiment. For sample collection during replication studies, 200 μl of TEC Plus medium was added to the apical surface, incubated for 10 min, and collected for plaque assay.

Immunofluorescence microscopy. Uninfected and infected FTE cells were washed three times with PBS for 10 min to remove mucus and fixed in 2% paraformaldehyde for 30 min. To analyze the distribution of sialic acid (SA) receptors, fixed FTE cells were blocked with 3% bovine serum albumin in PBS for 30 min and sequentially incubated with either biotinylated *Maackia amurensis* lectin I or II (MAA I and II; 20 μg/ml) or biotinylated *Sambucus nigra* lectin (SNA; 20 μg/ml) (Vector Laboratories, Burlingame, CA) or fluorescein isothiocyanate (FITC)-conjugated Jacalin (Vector) for 1 h, followed by the addition of FITC-conjugated avidin D (Vector Lab, Burlingame, CA). To characterize the ciliated cells and tight junctions, FTE cells were permeabilized with 0.5% Triton X-100 in PBS for 20 min and incubated with mouse anti-β-tubulin IV (Sigma, St. Louis, MO) or ZO-1, followed by rhodamine- or FITC-conjugated secondary antibody (Invitrogen, Carlsbad, CA). To detect influenza A virus antigen, infected FTE cells were fixed, permeabilized, blocked, and incubated with mouse anti-nucleoprotein (anti-NP) monoclonal antibody (A3) or rabbit anti-H5, anti-H1, or anti-H3 HA, followed by rhodamine- or FITC-conjugated secondary antibody. Immunostained cells were mounted with Vectashield mounting medium with 4′,6-diamidino-2-phenyindole (DAPI) and examined under a Zeiss Axioskop 2 fluorescence microscope.

Transmission electron microscopy (TEM). Differentiated FTE cells grown on transwell inserts were infected with influenza viruses at an MOI of 1 on the apical surface. At 24 h postinfection (p.i.), the cells were washed twice with PBS, fixed in 2.5% buffered glutaraldehyde for 1 h, and gamma irradiated (2×10^6 rad). Specimens were postfixed in 1% buffered osmium tetroxide, stained in 4% uranyl acetate, dehydrated, and embedded

in epoxy resin. Finally, ultrathin sections were cut and examined with a FEI Tecnai Spirit electron microscope.

Cell death enzyme-linked immunosorbent assay. FTE cells were infected with virus at an MOI of 1. At 48 h p.i., a cell death detection ELISAplus kit (Roche) was used for the quantitative determination of cytoplasmic histone-associated DNA fragments in both cell lysates (indicative of apoptosis) and supernatants (indicative of necrosis), according to the manufacturer's instructions.

Semiquantitative real-time PCR for ferret cytokine expression. Total RNA from virus-infected or uninfected cells was extracted using the RNeasy minikit (Qiagen, Carlsbad, CA) with DNase digestion, and 0.5 μg of total RNA was reverse transcribed with QuantiTect reverse transcription kit (Qiagen). The cDNA products were subjected to real-time PCR assay using QuantiTect SYBR green PCR kit (Qiagen) and analyzed with primer sets published previously (37).

Statistical data analysis. Student *t* test was performed on virus titers, cell death, and gene expression data.

RESULTS

Characterization of ferret tracheal differentiated primary epithelial cell cultures. FTE cells achieved high transepithelial resistance (>1,000 Ω·cm^2) after growing as liquid-covered cultures on transwell inserts for 2 to 3 days. After the apical medium was removed to create an air-liquid interface (ALI), increases in cilia formation and mucin-like secretions were observed over time of culture. After culturing for 3 weeks, we observed that the differentiated ferret cell cultures developed millimeter-sized patches in which the cilia spontaneously coordinated their beating in a circular pattern, rotating the surrounding mucus.

The differentiated FTE cell cultures were characterized using transmission electron microscopy (TEM) and immunofluorescence microscopy. TEM showed that FTE cultures consisted of basal cells on the membrane and ciliated and nonciliated cells reaching the apical surface (Fig. 1A). Cells were also stained with anti-β-tubulin IV (tubulin) antibody to identify ciliated cells, followed by DAPI (4′,6′-diamidino-2-phenylindole) staining for nucleus detection to quantify the total cell population. Ciliated cells were observed by visual inspection to cover more than 70% of the total surface area (Fig. 1B). Furthermore, tight junctions between cells close to the apical surface were observed by TEM (Fig. 1C) and by immunofluorescence staining using antibody against ZO-1, a protein that localizes specifically at tight junctions (Fig. 1D).

Next, we further characterized the distribution of ciliated and goblet-like cells on the apical surface using double immunofluorescent staining, followed by DAPI staining of nuclei (Fig. 1E). FTE cells derived from individual animals consisted of various percentages of ciliated cells. Using tubulin/DAPI staining, we manually examined more than 1,800 cells derived from four animals at a high magnification (×400). It was found that ciliated cells comprised, on average, 17% of the total cell population (range, 10 to 33% in cultures derived from 4 individual ferrets). Jacalin, a lectin that specifically binds to O-linked glycans mostly found in mucins secreted from goblet cells, was used to detect goblet-like cells (21, 28). Goblet-like cells were detected on the surface of 13% of the total cell population (range, 9 to 18% in cultures derived from four individual ferrets). However, as shown in the merged image, Jacalin was not detected on ciliated cells. The population of tubulin-and Jacalin-negative cells in FTE cultures may comprise of intermediate cells and basal cells (38). In summary, the differentiated FTE cells, maintained under ALI conditions, developed into a pseudostratified structure with tight junctions and contained at least three different cell types: ciliated epithelial cells, secretory cells, and basal cells.

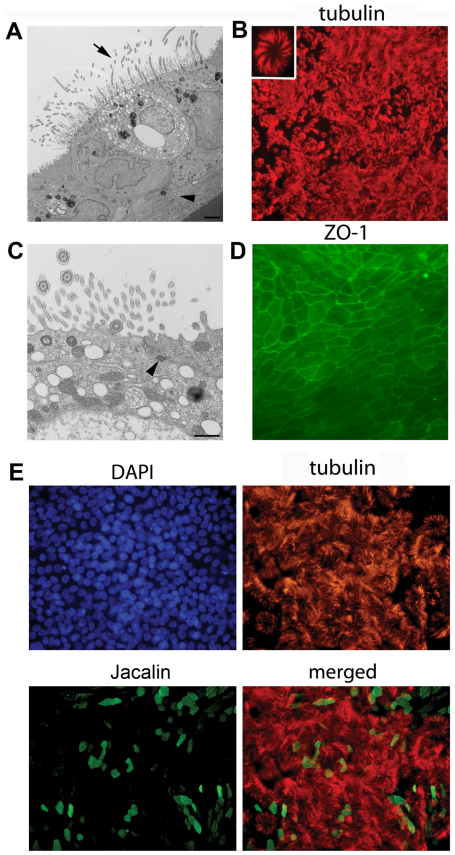

FIG 1 Structural characterization of ferret tracheal differentiated primary epithelial cell cultures (FTE) by TEM and immunofluorescence microscopy. (A) Multiple cell types in fully differentiated primary FTE cell cultures (TEM). The arrow marks a ciliated cell and the arrowhead, a basal cell. Scale bar, 2 μm. (B) Immunofluorescent staining of cilia using anti-β tubulin IV antibody (tubulin) (red) (magnification, ×100). An enlarged ciliated cell is shown in the inset. (C) Ultrastructure of a ciliated cell and a tight junction marked by an arrowhead (TEM). Bar, 500 nm. (D) Immunofluorescent staining of tight junctions using anti-ZO-1 antibody (green) (×400). (E) Characterization of cell surface markers on differentiated FTE cells. Double immunofluorescent staining of tubulin (red) and Jacalin (green) was performed in tandem with DAPI for nuclear staining (×400).

Distribution of α2,3- and α2,6-linked SA receptors on the apical surface. After determining that the apical surface of differentiated FTE cell cultures contained both ciliated and nonciliated cells, we next examined the distribution of SA receptors on the apical surface. Cells were stained with tubulin to identify ciliated cells and different plant lectins to detect receptors. The *Sambucus nigra* lectin (SNA) binds predominantly to α2,6-linked SA residues, and two isoforms of *Maackia amurensis* lectin (MAA I and MAA II) bind to α2,3-linked SA residues. MAA I is more specific toward SAα2,3Galβ1,4GlcNAc, and MAA II is specific toward SAα2,3Galβ1,3GalNAc (8). We manually examined more than 1,800 cells derived from four animals at a high magnification (×400). As illustrated in the merged images, we found that 95% of the α2,6-linked SA receptors were present on ciliated cells, and 5% were present on nonciliated cells. The α2,3-linked SA receptors

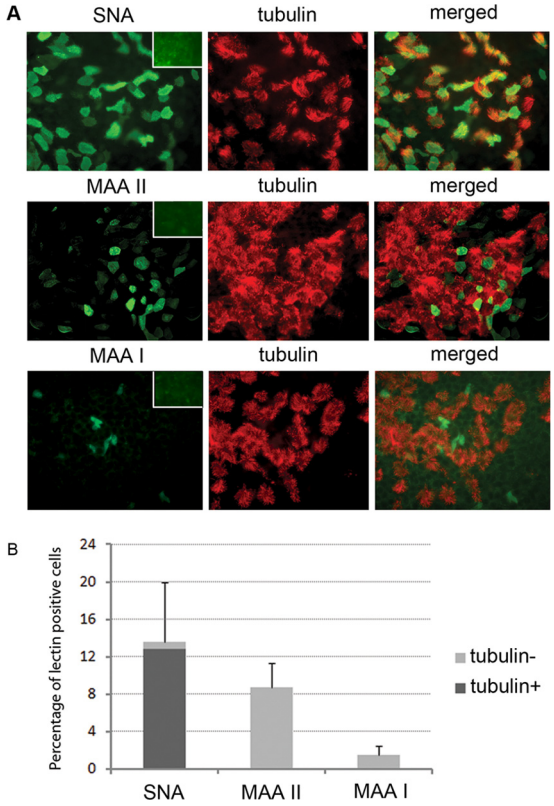

FIG 2 Distribution of α2,6-linked and α2,3-linked SA receptors on the surface of differentiated primary FTE cells. (A) Cells were stained (green) with SNA (which binds to α2,6-linked SA), and MAA I and II (specific for α2,3-linked SA), followed by cilia staining of tubulin (red) (×400). (B) Quantification of lectin staining on the surface of ciliated (tubulin+) and nonciliated (tubulin−) cells. Values represent the mean of the lectin-positive cells in cultures derived from six different animals with the standard deviation indicated.

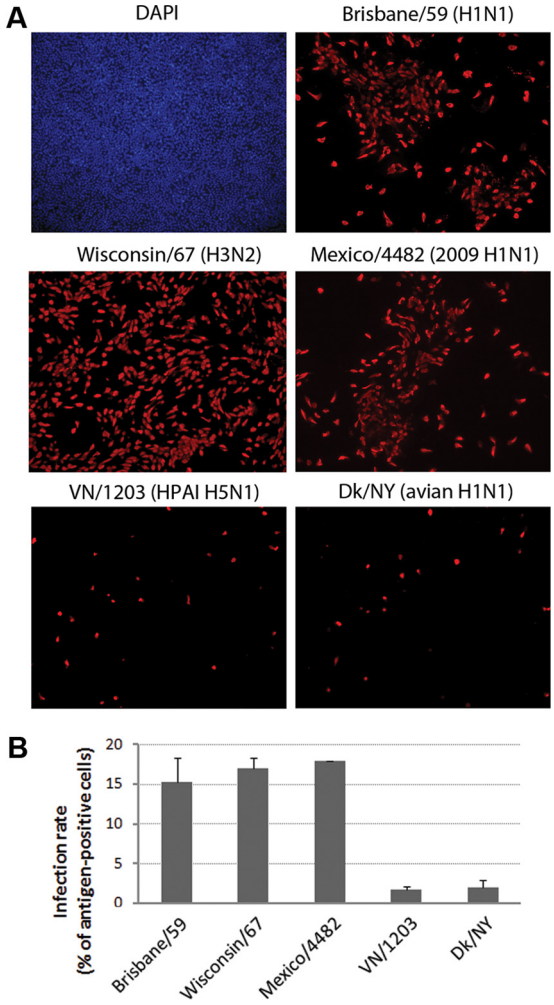

FIG 3 Influenza virus infection in differentiated primary FTE cells. FTE cells were infected with virus at an MOI of 1. Cells were fixed at 8 h p.i., stained for viral nuclear protein (NP, red), and compared to DAPI staining that indicated cellular nuclei (blue). (A) Immunofluorescent detection of influenza virus NP in infected cells (×100). (B) Quantification of NP-positive cells during infection. NP-positive cells and total cells were counted at higher magnification (×400) for the generation of infection rates. Values represent the mean of independent experiments from four different animals with the standard deviation indicated.

were exclusively present on nonciliated cells (Fig. 2A). Treatment of the apical surfaces of FTE cells with 25 mU/ml of neuraminidase for 1 h abolished all lectin staining (Fig. 2A, insets). The distribution of the receptors was analyzed further by counting more than 1,800 cells for the lectin-positive cells in cultures derived from six different ferrets. On average, 14% of cells were stained positive for SNA, 9% for MAA II, and 1.5% for MAA I (Fig. 2B). This finding obtained from multiple animals reinforces the greater density of ciliated cells with α2,6-linked SA in these cultures.

Infection and cellular tropism of human and avian influenza viruses. To test the permissiveness of FTE cells to influenza virus infection, cultures were inoculated apically with Brisbane/59 (H1N1), Wisconsin/67 (H3N2), Mexico/4482 (pdm2009 H1N1), VN/1203 (HPAI H5N1), or Dk/NY (avian H1N1) virus at an MOI of 1. The cells were fixed at 8 h p.i. and stained for influenza virus NP using DAPI for nuclei. The infection rate was quantified on more than 1,800 cells at a magnification of ×400 and is presented as the average percentage of cells that were NP positive relative to total cell population from the infection of cultures derived from four individual animals. In general, human influenza viruses infected FTE cells more efficiently than avian influenza viruses, including VN/1203 virus (Fig. 3A). Infection rates for the three human influenza viruses ranged from 15 to 18%, which was significantly higher than that for avian influenza viruses, which ranged from 1.5 to 2.4% ($P < 0.01$) (Fig. 3B).

We next characterized the cellular tropism of two human viruses and one avian influenza virus using double-immunofluorescence staining. FTE cells were infected apically with influenza virus at an MOI of 1, and the cells were fixed at 8 h p.i. and stained for viral antigen (HA or NP) and cell surface markers (tubulin or Jacalin). Cellular tropism for influenza virus infection was quantified by counting HA/tubulin- and NP/Jacalin-positive cells from infected cultures derived from four individual animals. Human influenza viruses, Wisconsin/67 and Brisbane/59, mainly infected ciliated cells (95%) and, to a much lesser extent, nonciliated cells (5%), including both Jacalin-positive and -negative cells (Fig. 4). In contrast, VN/1203 virus exclusively infected nonciliated cells, including both Jacalin-positive and -negative cells, but at a much lower infection rate of 1.5 to 1.8%.

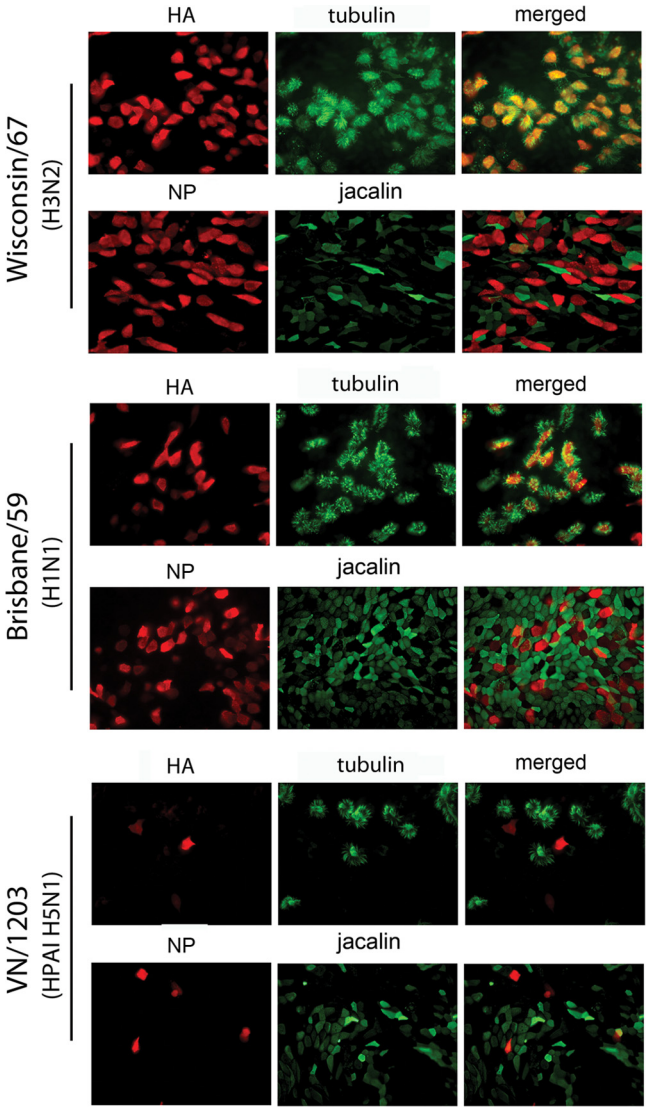

FIG 4 Cellular tropism of influenza virus infection in differentiated primary FTE cells. Cells were infected apically with virus at an MOI of 1 and fixed at 8 h p.i. Cells were stained to identify influenza virus HA or NP (red) and to identify ciliated cells (tubulin, green) and secretory cells (Jacalin, green) (×400).

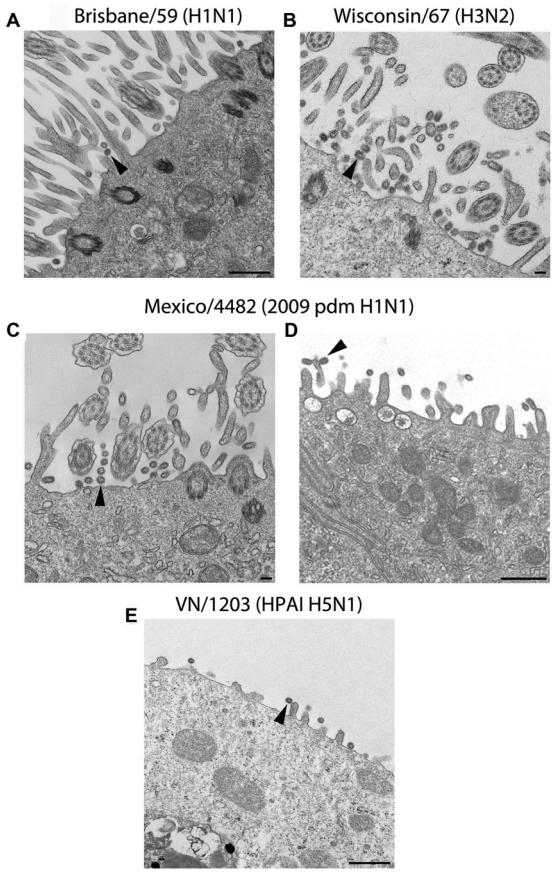

FIG 5 TEM demonstrates the release and cellular tropism of influenza virus. Differentiated primary FTE cells were infected apically with virus at an MOI of 1 and fixed at 24 h p.i. Spherical virions are shown by the arrowhead. Scale bars, 500 nm (A, D, and E) and 100 nm (B and C).

Cellular tropism and the release of influenza virus from infected cells was further investigated using TEM. FTE cells were infected apically with influenza viruses at an MOI of 1 and examined for virus release at 24 h p.i. In general, a greater number of infected cells were detected during human influenza virus infection than during avian virus infection. The Brisbane/59, Mexico/4482, and Wisconsin/67 viruses were predominantly released from the apical surface membranes of ciliated cells (Fig. 5A to C). However, the release of virus from at least one nonciliated cell was detected during Mexico/4482 virus infection (Fig. 5D). In contrast, the apical release of VN/1203 virus was detected only from nonciliated cells, albeit only sporadically (Fig. 5E). No infected cells were identified by TEM during Dk/NY virus infection because of the very low infection rate.

Replication of human and avian influenza virus. We compared the replication kinetics of all five influenza viruses. Cells were infected apically with virus at an MOI of 0.01 in triplicate, with each culture representing an individual animal. As shown in Fig. 6A, all human viruses reached high titers at 24 h p.i.; the titer of Mexico/4428 virus (10^7 PFU/ml) was significantly higher ($P < 0.05$). For VN/1203 virus, despite its much lower initial infection rate at 8 h p.i. (Fig. 3), this HPAI H5N1 virus replicated to a mean peak titer of 10^6 PFU/ml at 24 h p.i., comparable to titers attained by human virus infection (10^5 to 10^7 PFU/ml). Dk/NY virus replicated less efficiently, reaching a virus titer of 10^4 PFU/ml at 24 h p.i., which was significantly lower than for all of the other viruses tested ($P < 0.05$). However, by 48 h p.i. this avian H1N1 virus reached titers comparable to the other viruses.

Next, the recovery of virus from the apical versus the basolateral surfaces of cells was evaluated. Brisbane/59, Mexico/4482, Wisconsin/67, and Dk/NY viruses were released exclusively from the apical surface for all times examined, and the titers of Brisbane/59 virus from the apical and basolateral surfaces are displayed as representative of the findings for the four viruses tested (Fig. 6B). In contrast, VN/1203 virus was detected not only from the apical side but also from the basolateral side, as early as 24 h p.i.; virus isolated from the basolateral side reached a mean peak titer of 10^4PFU/ml at 48 h p.i., indicating a unique virulence attribute of this HPAI H5N1 virus (Fig. 6B).

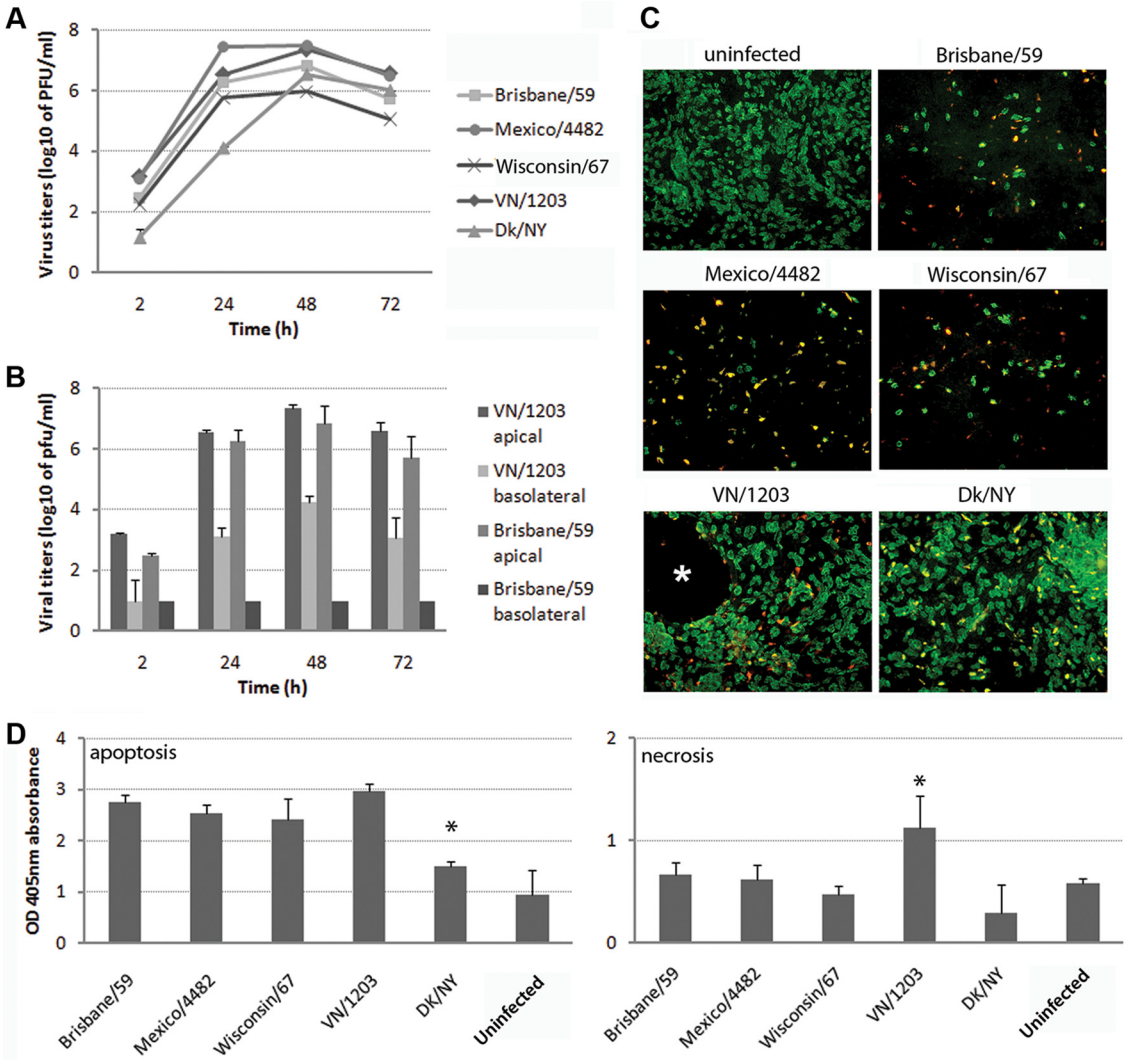

FIG 6 Replication of influenza virus in differentiated primary FTE cells. The experiment was done in triplicate with cells from three individual animals. Cells were infected apically with virus at an MOI of 0.01. Cell supernatants were collected at the indicated time points from both apical and basolateral sides of the monolayer, and virus titers were determined by plaque assay. Values represent the mean of three independent wells with the standard deviation indicated. (A) Replication kinetics of influenza virus (both apical and basolateral sides). (B) Assessment of virus recovered from either apical or basolateral side. (C) Evaluation of the integrity of the infected monolayer and the presence of ciliated cells. FTE cells were infected with virus at an MOI of 0.01 and fixed at 120 h p.i. Cells were stained to identify influenza virus NP (yellow) and ciliated cells (tubulin, green) (×100). A white asterisk indicates the damaged area of the monolayer. (D) Determination of cell death during influenza virus infection in differentiated FTE cells. Cells were infected apically with virus at an MOI of 1, and the cell lysates and supernatants were analyzed to determine the level of apoptosis and necrosis, respectively. Values (absorbance) represent the mean of three independent treatments with standard deviation indicated. Significantly higher necrosis induced by VN/1203 virus is noted (*, $P < 0.01$).

Finally, the relationship between infection and the loss of cilia was examined at later times postinfection. FTE cells infected at an MOI of 0.01 were fixed at 120 h p.i. for double-immunofluorescence staining to indicate viral NP (shown in yellow) and ciliated cells (tubulin, shown in green). As shown previously (Fig. 4 and 5), human viruses mainly targeted ciliated cells, whereas avian viruses infected nonciliated cells. Compared to uninfected cell cultures, infection with human influenza viruses resulted in extensive loss of cilia as determined by tubulin staining (Fig. 6C). In contrast, FTE cells infected with the avian viruses, VN/1203 and Dk/NY, maintained levels of ciliated cells comparable to uninfected cultures. The integrity of the cell monolayers was also examined during influenza virus infection. Cells infected with human viruses and Dk/NY virus retained their integrity up to 120 h p.i., whereas the cell cultures infected with HPAI VN/1203 virus exhibited increased cytopathic effect (CPE) at 24 h p.i. and significant CPE at 48 h p.i., with substantial destruction of the cell monolayer at 120 h p.i. (Fig. 6C). This may result in diffusion of the virus into the basolateral side after the destruction of tight junctions in H5N1 virus-infected cultures.

Cell death during influenza virus infection. Cell death (apoptosis and necrosis) resulting from influenza virus infection usually damages the epithelium. In the previous experiment, we observed a loss of cellular integrity during VN/1203 virus infection (Fig. 6C). To examine cell death during influenza virus infection, FTE cells were infected with virus at an MOI of 1, and the levels of cytoplasmic histone-associated DNA fragments were quantified at 48 h p.i. in cell lysates (apoptosis) and in culture supernatants

(necrosis). Infection with the Brisbane/59, Mexico/4482, Wisconsin/67, and VN/1203 viruses resulted in comparable levels of apoptosis, which were 2.5 to 3 times higher than in uninfected samples, whereas the level of apoptosis after infection with Dk/NY virus was significantly lower than those of the other viruses ($P < 0.001$), and only ~1.5 times higher than in uninfected samples (Fig. 6D). The levels of cell necrosis were low overall; however, the level for VN/1203 was significantly higher than for all other viruses ($P < 0.05$) (Fig. 6D), which may be responsible for the monolayer damage and virus diffusion to the basolateral side observed (Fig. 6B and C).

Expression of immune mediator genes during influenza virus infection. High viral load and exacerbated cytokine production in the respiratory tract of humans infected with HPAI H5N1 have been shown to be associated with severe disease outcomes (4). We compared innate immune responses in FTE cells elicited by infection with different influenza viruses. The cells were infected apically with virus at an MOI of 1 in triplicate, with each culture representing an individual animal. Total RNA was collected at 24 h p.i. to assess gene expression using real-time PCR. As shown in Fig. 7A, M1 gene expression levels varied slightly among viruses following infection, with Mexico/4482 virus having the highest expression, and Dk/NY virus, the lowest. Interestingly, VN/1203 virus resulted in an M1 gene level at 24 h p.i. comparable to those of human viruses, even though its initial infection rate at 8 h p.i. was 10 times lower than for those viruses. (Fig. 3).

Next, the transcriptional levels of 16 ferret immune mediator genes—including the genes coding for alpha interferon (IFN-α), IFN-β, IFN-γ, interleukin-2 (IL-2), IL-4, IL-6, IL-8, IL-10, IL-12, tumor necrosis factor alpha (TNF-α), CXCL9, CXCL10, CXCL11, IL-1α, IL-1β, and CXCR3—were examined by real-time PCR using GAPDH (glyceraldehyde-3-phosphate dehydrogenase) as an internal control. Five genes were highly induced during infection (Fig. 7B), whereas another five were moderately induced (Fig. 7C). No induction was detected for IL-2, IL-4, IL-10, IL-12, IL-1α, and IL-1β. In general, VN/1203 virus induced the highest transcriptional levels of IFN-α, IFN-β, IFN-γ, TNF-α, CXCL9, CXCL10, CXCL11, IL-6, and IL-8, and Dk/NY virus induced the lowest levels. During VN/1203 virus infection, the gene transcriptional levels of three CXC chemokines—CXCL9, CXCL10, and CXCL11—were significantly higher than for all other viruses ($P < 0.05$). *In vivo*, these chemokines serve as chemoattractants for various types of leukocytes to the affected region. Their receptor, CXCR3, was also slightly induced during influenza virus infection. During infection with human viruses, slight variations were observed at the transcriptional level. Mexico/4482 virus induced higher levels of gene expression of IFN-β, TNF-α, and IL-6 but lower levels of CXCL9, CXCL10, and CXCL11 than did the other two human viruses. Taken together, HPAI H5N1 virus infection induced higher levels of proinflammatory mediators compared to other viruses, which may be associated with the pathogenesis observed in infected ferrets.

The impact of temperature and different tracheal sections on the replication of influenza virus. Previous studies have suggested a correlation between the transmissibility of influenza viruses in ferrets and their ability to replicate efficiently at the lower temperature (33°C) found in the environment of mammalian upper airway (17). We evaluated the replication kinetics of influenza virus in FTE cells that were cultured at either 33°C or at the standard 37°C culture condition. Brisbane/59 and VN/1203 were selected to represent human and avian influenza viruses, respectively. As shown in Fig. 8A, Brisbane/59 virus replicated equally well at both temperatures and reached similar titers at all time points examined. However, VN/1203 virus did not replicate as well at 33°C compared to 37°C, with significantly lower titers at both 24 h and 48 h p.i. ($P < 0.05$). Moreover, reduced CPE and less cellular destruction were observed in cultures at 33°C compared to FTE cells grown at 37°C (not shown). These results demonstrate that H5N1 virus does not replicate as well as human influenza viruses at the lower temperatures found in the upper airway of mammals.

Studies on the distribution of influenza virus receptors in the respiratory tract have suggested that human viruses replicate well in the upper respiratory tract, whereas avian viruses mostly target the lower respiratory tract (2, 10). To examine

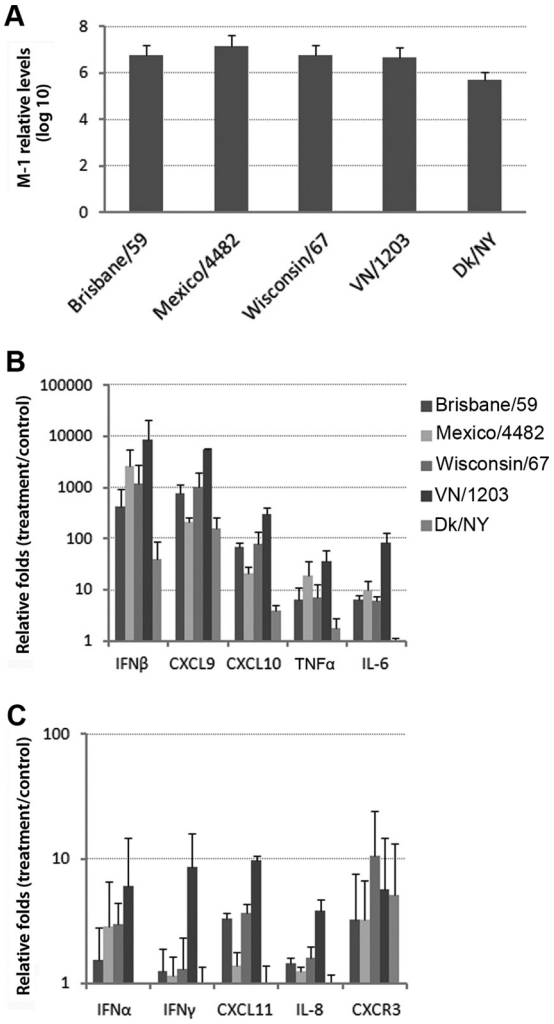

FIG 7 Evaluation of host immune mediator expression to influenza virus infection in differentiated primary FTE cells. The experiment was done in triplicate with cells from three individual animals. Cells were infected apically with virus at an MOI of 1, and RNA was extracted at 24 h p.i. and examined by real-time PCR. (A) Expression of M1 viral gene in infected cells. (B and C) Expression of immune mediator genes during influenza virus infection. Values represent the mean of three independent treatments with the standard deviation indicated.

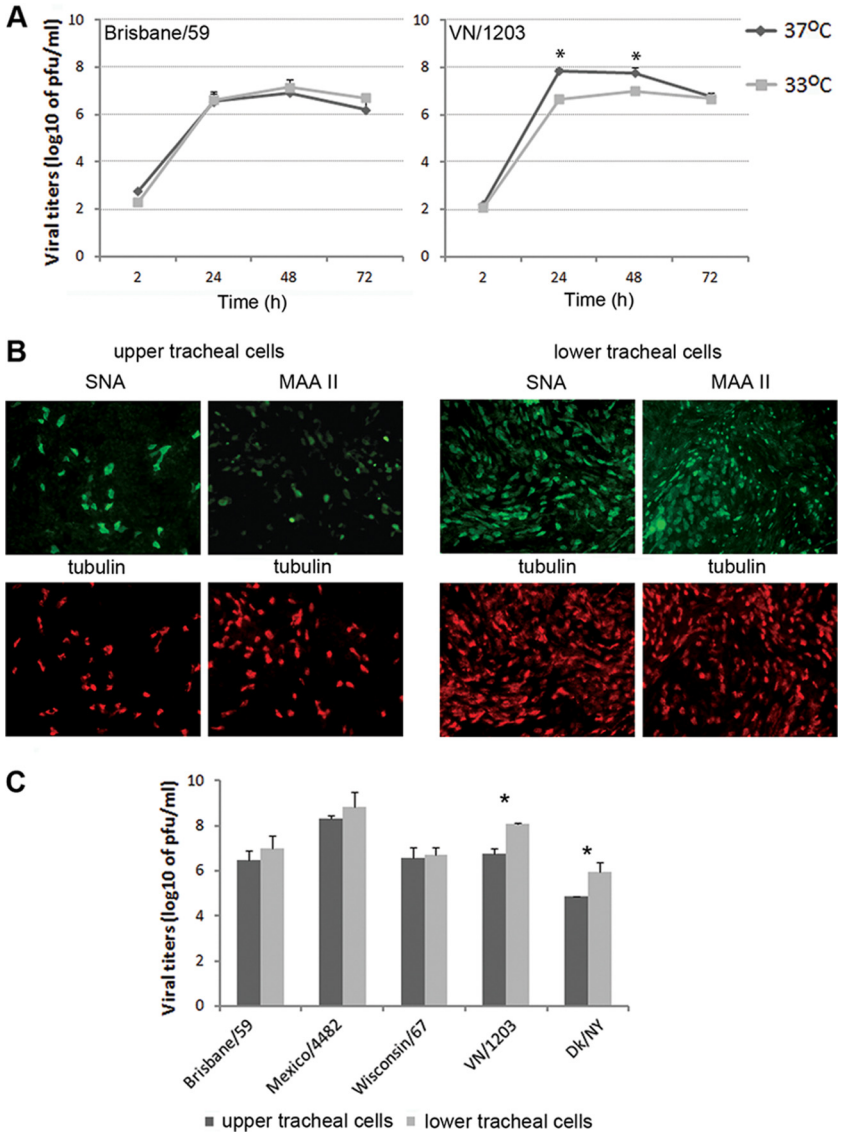

FIG 8 Evaluation of virus replication at different temperature and in FTE cells derived from different portion of trachea. (A) Comparison of virus replication at 37 and 33°C. Asterisks indicate statistically significant differences in virus titer between the two temperatures. (B) Staining of lectins (green) and tubulin (red) on FTE cells isolated from the upper half and lower half of the trachea (×100). DAPI staining showed monolayers with similar confluences for these cultures (data not shown). (C) Comparison of virus replication in upper and lower FTE cells. The images shown represent three individual ferrets. The significance is noted (*, $P < 0.05$) in virus titers of avian viruses between upper and lower tracheal cells.

tissue tropism of influenza virus in the ferret trachea, FTE cells were isolated from either the upper half or the lower half of the trachea and cultured separately. FTE cells were cultured as previously described and stained with SNA lectin for α2,6-linked SA residues or MAA II lectin for α2,3-linked SA residues, followed by staining with tubulin to identify ciliated cells. Compared to upper FTE cultures, lower FTE cultures had more ciliated cells and more α2,3- and α2,6-linked SA receptors (Fig. 8B). Next, we compared the replication of all five influenza viruses between upper and lower FTE cultures. The cells were infected at an MOI of 0.01, and virus titers were measured at 24 h p.i. As shown in Fig. 8C, avian viruses (VN/1203 and Dk/NY) reached significantly higher titers in lower FTE cultures compared to upper FTE cultures. In contrast, there were no significant differences in human virus titers between the upper and lower FTE cultures.

DISCUSSION

The pathogenesis and transmission of influenza virus has been intensively investigated recently in the ferret model (18, 39). However, the cellular and molecular characteristics of influenza virus-host interactions occurring in the airway of this species are largely unknown. Here, we provide data on the cellular tropism and infectivity of influenza virus in ferret tracheal differentiated primary epithelial cell cultures. *In vitro*, the primary FTE cells cultured at the air-liquid interface developed to a pseudostratified structure consisting of tight junctions and three different types of epithelial cells: ciliated, secretory, and basal cells. In these cultures, we found

that 95% of α2,6-linked SA receptors were present on ciliated cells and that α2,3-linked SA receptors were exclusively present on nonciliated cells. We demonstrated that human viruses predominantly infected ciliated cells at a high infection rate, whereas avian influenza viruses exclusively infected nonciliated cells at a much lower infection rate. The low-path avian H1N1 virus replicated less efficiently compared to the human influenza viruses; however, HPAI H5N1 virus replicated to titers similar to those obtained with the human influenza virus subtypes. H5N1 virus infection resulted in substantial necrosis and destruction of the cell monolayer, resulting in recovery of virus from the basolateral side. *In vivo*, destruction of the cell monolayer would presumably allow virus spread from the epithelia to underlying tissues. H5N1 virus infection of FTE cells also induced high levels of proinflammatory cytokines and chemokines, a finding consistent with exacerbated innate responses associated with severe H5N1 disease in humans and the ferret model (4, 37, 40, 41).

Airway epithelial cell-specific tropism of influenza viruses was observed in differentiated FTE cells. Consistent with our results, an early study that examined infected ferret tracheal explants using TEM found that H3N2 virus (A/Victoria/3/75) predominantly attached to ciliated cells (77 to 87%), with a much smaller proportion attaching to nonciliated cells (1 to 9%) (42). Moreover, after examining ferret trachea and bronchus tissues using lectin staining, Xu et al. reported that α2,6-linked SA receptors were predominantly associated with ciliated cells (22). However, there are conflicting reports regarding the presence of sialic acid receptors for influenza viruses on human airway cells. Early work demonstrated that human influenza viruses bind to ciliated cells displaying α2,6-linked SA and α2,3-linked SA receptors were found on nonciliated cuboidal bronchiolar cells (5–7, 10, 11, 13, 42) but rarely on ciliated cells. Subsequently, it has been shown that goblet cells also express α2,6-linked SA receptors (8), and the human-adapted 1918 HA demonstrated substantial binding to goblet cell regions of human tracheal tissue (21, 43). Conversely, studies using human tracheal epithelial cell cultures have shown that human influenza viruses infected both nonciliated cells and ciliated cells (25, 29) and that avian influenza viruses were predominantly localized on ciliated cells (9, 25, 26, 29, 30). The reasons for the discrepancies in cellular tropism of influenza virus between our *in vitro* model of ferret tracheal differentiated epithelial cells and those found in human tracheal epithelial cells are not clear. First, we cannot exclude the possibility that a species difference in cellular tropism of influenza virus exists between ferrets and humans. Moderate differences in receptor distribution and viral tropism have been observed between ferret and human tracheal tissue using lectin/Jacalin staining and viral attachment analysis (21). Second, different human and avian influenza virus strains used in these studies may possess different binding patterns to SA-containing carbohydrates, which can lead to variance observed in cellular tropism. Third, the primary ferret epithelial cells that we used were seeded onto transwells immediately after enzymatic cell dissociation without further passaging and manipulation. In human cell cultures, cells are typically passaged *in vitro* at least three times, and the ciliated cells are reinduced under ALI culture conditions.

The finding that human influenza viruses mainly infected ciliated cells in our primary FTE cell model, on which α2,6-linked SA receptors predominate, is consistent with the tissue tropism of seasonal influenza viruses, which infect mainly the upper respiratory tract of humans and ferrets (2, 9, 10). FTE cultures may not be able to recapture the apparent higher density of ciliated cells present in the native ferret trachea (33), which may result in differences in sialic acid distribution. In comparison to our FTE cells, Jayaraman et al. (21) demonstrated apparently less MAA-II lectin staining (for avian influenza virus receptors) on ferret tissues sections. In the upper respiratory tract, ciliated cells are abundant at the luminal surface of the trachea, consisting of 30 to 50% of the total epithelial population in the tracheal (44). Among the human viruses tested, the 2009 pandemic H1N1 virus, Mexico/4482, replicated to significantly higher titers than seasonal H1N1 and H3N2 viruses in FTE cells, which is consistent with the increased pathogenicity observed in ferrets (15). Interestingly, the loss of cilia from ciliated cells was observed during the course of infection with human influenza viruses but not with the avian influenza viruses. In spite of the loss of cilia during virus infection, the integrity of the monolayer was retained. Destruction of cilia has been observed previously following infection of ferret tracheal organ culture with human influenza viruses that were associated with excess mortality in epidemiological studies (45). In general, effective mucociliary clearance requires normal ciliary activity and mucus production, which represents an essential line of defense against inhaled agents (46). The mechanisms underlying influenza virus-induced ciliary damage or loss of cilia are not well understood but may be due, at least in part, to apoptosis, which we observed in infected cells at 48 h p.i. Additional studies are required to fully elucidate the relationship between loss of cilia and virulence during influenza virus infection.

During HPAI H5N1 virus infection, ferrets present disease progression (16, 47) similar to the clinical course in humans, including the progression to severe lower respiratory tract disease and extrapulmonary complications, including multiorgan failure in fatal cases (4, 40, 41). H5N1 virus targets the lower respiratory tract, especially lung tissues, largely due to the predominance of α2,3-linked SA receptors (2, 14). However, it has been shown that H5N1 viruses are capable of infecting human upper respiratory tract tissues, such as nasopharyngeal, adenoid, and tonsillar tissues, as demonstrated in *ex vivo* cultures (12). In our study, we found that avian influenza viruses replicated more efficiently in FTE cells derived from the lower trachea than in cells derived from the upper trachea, which correlated with increased expression of α2,3-linked SA receptors in the lower trachea. However, regardless of the tissue location, H5N1 virus replicated as efficiently as human influenza viruses in ferret tracheal cells despite its low initial infection rate. We found that H5N1 virus predominantly infected nonciliated cells and resulted in significantly more necrosis and substantial damage to the epithelial layer, which may contribute to the loss of cell integrity and diffusion of virus to the basolateral surface of tracheal epithelium. *In vivo*, recovery of virus from the epithelial basolateral side would contribute to infection of other cell types, including endothelial cells which possess α2,3-linked SA receptors (48), and virus spread to tissues outside of respiratory tract, potentially contributing to disease progression in mammals.

Innate immunity to influenza virus is the front line of host defense. However, in patients infected by H5N1 virus, the intense inflammatory response to infection may contribute to disease pathogenesis, further complicating recovery (4, 40, 41). Compared to human influenza virus infection, significantly higher levels of IP-10, MCP-1, MIG, IL-6, IL-8, IL-10, and IFN-γ have been detected in humans infected with H5N1 virus, especially in fatal

cases (4). In ferrets, selected cytokine responses to influenza virus have been studied on a limited basis using gene expression analysis of respiratory tract tissues (37, 49, 50). Similar to results observed in humans, elevated levels of proinflammatory cytokine and chemokine mRNAs have been observed in ferret lungs infected with H5N1 viruses. In our FTE system, with the exception of avian H1N1 virus, all subtypes of influenza virus tested induced high levels of IFN-β, CXCL9 (MIG), CXCL10 (IP-10), TNF, and IL-6, but HPAI H5N1 virus elicited the highest levels of cytokines despite a lower infection rate compared to human influenza viruses.

One human host factor that may limit zoonotic transmission of avian influenza viruses is the temperature restriction of these viruses. Previously, we found an association between influenza viruses that are highly transmissible in ferrets and their ability to replicate efficiently at 33°C (17). In the human airway, surface temperatures range from 32 ± 0.05°C in the upper trachea to 35.5 ± 0.3°C in the subsegmental bronchi during quiet breath (51). In contrast, avian influenza viruses replicate at 40 to 41°C in the avian enteric tract and replicate less efficiently at cooler temperatures, limiting their ability to infect the upper respiratory tract of mammalian species. This inefficient viral replication at 33°C in mammalian cells has been linked to the viral polymerase subunit, PB2, especially amino position 627 (52). In addition to the PB2 gene, avian-like surface glycoproteins (HA or NA) may also contribute to the temperature restriction of avian viruses (28). In differentiated FTE cells, we found that human viruses infect and replicate efficiently at both 37 and 33°C, whereas VN/1203 virus, which possesses a lysine at position 627, replicated less efficiently at 33°C. The H5N1 virus was unique in its inability to replicate well at the lower temperature (33°C) compared to its ability to replicate at the higher temperature (37°C). This may partially explain the paucity of H5N1 virus transmission observed in ferrets and humans (53, 54).

Differentiated primary FTE cell cultures represent features of the ferret trachea epithelium and provide a valuable *in vitro* model to study influenza virus tropism and host interaction during infection. This model reflects the pathogenesis phenotype and virus replication observed in the animal model and contributes to the understanding of the disease progression at the airway cellular level. The FTE system highlights several features of HPAI H5N1 viruses that may contribute to their virulence *in vivo*, including a relatively higher virus load at lower airway temperatures, a heightened inflammatory mediator response, notable cell death, and recovery of virus at the basolateral cell surface. Future studies on the interaction between influenza virus-induced inflammation, cell tropism and the ferret tracheal epithelium, especially in *ex vivo* and *in vivo* models, is warranted.

ACKNOWLEDGMENTS

We thank Mary McCauley for scientific editing, Hongquan Wan for discussion of culture techniques, Jack Harkema for reference, and Xiuhua Lu for reagents.

The findings and conclusions in this report are those of the authors and do not necessarily represent the views of the Centers for Disease Control and Prevention.

REFERENCES

1. **Monto AS, Gravenstein S, Elliott M, Colopy M, Schweinle J.** 2000. Clinical signs and symptoms predicting influenza infection. Arch. Intern. Med. **160**:3243–3247.
2. **Shinya K, Ebina M, Yamada S, Ono M, Kasai N, Kawaoka Y.** 2006. Avian flu: influenza virus receptors in the human airway. Nature **440**:435–436.
3. **Abdel-Ghafar AN, Chotpitayasunondh T, Gao Z, Hayden FG, Nguyen DH, de Jong MD, Naghdaliyev A, Peiris JS, Shindo N, Soeroso S, Uyeki TM.** 2008. Update on avian influenza A (H5N1) virus infection in humans. N. Engl. J. Med. **358**:261–273.
4. **de Jong MD, Simmons CP, Thanh TT, Hien VM, Smith GJ, Chau TN, Hoang DM, Chau NV, Khanh TH, Dong VC, Qui PT, Cam BV, QHa do, Guan Y, Peiris JS, Chinh NT, Hien TT, Farrar J.** 2006. Fatal outcome of human influenza A (H5N1) is associated with high viral load and hypercytokinemia. Nat. Med. **12**:1203–1207.
5. **Baum LG, Paulson JC.** 1990. Sialyloligosaccharides of the respiratory epithelium in the selection of human influenza virus receptor specificity. Acta Histochem. Suppl. **40**:35–38.
6. **Couceiro JN, Paulson JC, Baum LG.** 1993. Influenza virus strains selectively recognize sialyloligosaccharides on human respiratory epithelium; the role of the host cell in selection of hemagglutinin receptor specificity. Virus Res. **29**:155–165.
7. **Gagneux P, Cheriyan M, Hurtado-Ziola N, van der Linden EC, Anderson D, McClure H, Varki A, Varki NM.** 2003. Human-specific regulation of alpha 2-6-linked sialic acids. J. Biol. Chem. **278**:48245–48250.
8. **Nicholls JM, Bourne AJ, Chen H, Guan Y, Peiris JS.** 2007. Sialic acid receptor detection in the human respiratory tract: evidence for widespread distribution of potential binding sites for human and avian influenza viruses. Respir. Res. **8**:73.
9. **Shelton H, Ayora-Talavera G, Ren J, Loureiro S, Pickles RJ, Barclay WS, Jones IM.** 2011. Receptor binding profiles of avian influenza virus hemagglutinin subtypes on human cells as a predictor of pandemic potential. J. Virol. **85**:1875–1880.
10. **van Riel D, den Bakker MA, Leijten LM, Chutinimitkul S, Munster VJ, de Wit E, Rimmelzwaan GF, Fouchier RA, Osterhaus AD, Kuiken T.** 2010. Seasonal and pandemic human influenza viruses attach better to human upper respiratory tract epithelium than avian influenza viruses. Am. J. Pathol. **176**:1614–1618.
11. **van Riel D, Munster VJ, de Wit E, Rimmelzwaan GF, Fouchier RA, Osterhaus AD, Kuiken T.** 2007. Human and avian influenza viruses target different cells in the lower respiratory tract of humans and other mammals. Am. J. Pathol. **171**:1215–1223.
12. **Nicholls JM, Chan MC, Chan WY, Wong HK, Cheung CY, Kwong DL, Wong MP, Chui WH, Poon LL, Tsao SW, Guan Y, Peiris JS.** 2007. Tropism of avian influenza A (H5N1) in the upper and lower respiratory tract. Nat. Med. **13**:147–149.
13. **van Riel D, Kuiken T.** 2012. The role of cell tropism for the pathogenesis of influenza in humans. Future Virol. **7**:295–307.
14. **van Riel D, Munster VJ, de Wit E, Rimmelzwaan GF, Fouchier RA, Osterhaus AD, Kuiken T.** 2006. H5N1 virus attachment to the lower respiratory tract. Science **312**:399.
15. **Maines TR, Jayaraman A, Belser JA, Wadford DA, Pappas C, Zeng H, Gustin KM, Pearce MB, Viswanathan K, Shriver ZH, Raman R, Cox NJ, Sasisekharan R, Katz JM, Tumpey TM.** 2009. Transmission and pathogenesis of swine-origin 2009 A(H1N1) influenza viruses in ferrets and mice. Science **325**:484–487.
16. **Maines TR, Lu XH, Erb SM, Edwards L, Guarner J, Greer PW, Nguyen DC, Szretter KJ, Chen LM, Thawatsupha P, Chittaganpitch M, Waicharoen S, Nguyen DT, Nguyen T, Nguyen HH, Kim JH, Hoang LT, Kang C, Phuong LS, Lim W, Zaki S, Donis RO, Cox NJ, Katz JM, Tumpey TM.** 2005. Avian influenza (H5N1) viruses isolated from humans in Asia in 2004 exhibit increased virulence in mammals. J. Virol. **79**:11788–11800.
17. **Van Hoeven N, Pappas C, Belser JA, Maines TR, Zeng H, Garcia-Sastre A, Sasisekharan R, Katz JM, Tumpey TM.** 2009. Human HA and polymerase subunit PB2 proteins confer transmission of an avian influenza virus through the air. Proc. Natl. Acad. Sci. U. S. A. **106**:3366–3371.
18. **Belser JA, Katz JM, Tumpey TM.** 2011. The ferret as a model organism to study influenza A virus infection. Dis. Model Mech. **4**:575–579.
19. **Chutinimitkul S, van Riel D, Munster VJ, van den Brand JM, Rimmelzwaan GF, Kuiken T, Osterhaus AD, Fouchier RA, de Wit E.** 2010. In vitro assessment of attachment pattern and replication efficiency of H5N1 influenza A viruses with altered receptor specificity. J. Virol. **84**:6825–6833.
20. **Maher JA, DeStefano J.** 2004. The ferret: an animal model to study influenza virus. Lab Anim. **33**:50–53.
21. **Jayaraman A, Chandrasekaran A, Viswanathan K, Raman R, Fox JG,**

Sasisekharan R. 2012. Decoding the distribution of glycan receptors for human-adapted influenza a viruses in ferret respiratory tract. PLoS One **7**:e27517. doi:10.1371/journal.pone.0027517.
22. **Xu Q, Wang W, Cheng X, Zengel J, Jin H.** 2010. Influenza H1N1 A/Solomon Island/3/06 virus receptor binding specificity correlates with virus pathogenicity, antigenicity, and immunogenicity in ferrets. J. Virol. **84**:4936–4945.
23. **Kirkeby S, Martel CJ, Aasted B.** 2009. Infection with human H1N1 influenza virus affects the expression of sialic acids of metaplastic mucous cells in the ferret airways. Virus Res. **144**:225–232.
24. **Chan MC, Chan RW, Yu WC, Ho CC, Yuen KM, Fong JH, Tang LL, Lai WW, Lo AC, Chui WH, Sihoe AD, Kwong DL, Wong DS, Tsao GS, Poon LL, Guan Y, Nicholls JM, Peiris JS.** 2010. Tropism and innate host responses of the 2009 pandemic H1N1 influenza virus in ex vivo and in vitro cultures of human conjunctiva and respiratory tract. Am. J. Pathol. **176**:1828–1840.
25. **Ibricevic A, Pekosz A, Walter MJ, Newby C, Battaile JT, Brown EG, Holtzman MJ, Brody SL.** 2006. Influenza virus receptor specificity and cell tropism in mouse and human airway epithelial cells. J. Virol. **80**:7469–7480.
26. **Matrosovich MN, Matrosovich TY, Gray T, Roberts NA, Klenk HD.** 2004. Human and avian influenza viruses target different cell types in cultures of human airway epithelium. Proc. Natl. Acad. Sci. U. S. A. **101**:4620–4624.
27. **Rowe RK, Brody SL, Pekosz A.** 2004. Differentiated cultures of primary hamster tracheal airway epithelial cells. In Vitro Cell Dev. Biol. Anim. **40**:303–311.
28. **Scull MA, Gillim-Ross L, Santos C, Roberts KL, Bordonali E, Subbarao K, Barclay WS, Pickles RJ.** 2009. Avian influenza virus glycoproteins restrict virus replication and spread through human airway epithelium at temperatures of the proximal airways. PLoS Pathog. **5**:e1000424. doi:10.1371/journal.ppat.1000424.
29. **Thompson CI, Barclay WS, Zambon MC, Pickles RJ.** 2006. Infection of human airway epithelium by human and avian strains of influenza A virus. J. Virol. **80**:8060–8068.
30. **Wan H, Perez DR.** 2007. Amino acid 226 in the hemagglutinin of H9N2 influenza viruses determines cell tropism and replication in human airway epithelial cells. J. Virol. **81**:5181–5191.
31. **Xing Z, Harper R, Anunciacion J, Yang Z, Gao W, Qu B, Guan Y, Cardona CJ.** 2011. Host immune and apoptotic responses to avian influenza virus H9N2 in human tracheobronchial epithelial cells. Am. J. Respir. Cell Mol. Biol. **44**:24–33.
32. Lenfant C (ed). 2003. Lung biology in health and disease, vol 81. Marcel Dekker, Inc, New York, NY.
33. **Liu X, Luo M, Zhang L, Ding W, Yan Z, Engelhardt JF.** 2007. Bioelectric properties of chloride channels in human, pig, ferret, and mouse airway epithelia. Am. J. Respir. Cell Mol. Biol. **36**:313–323.
34. **U. S. Department of Agriculture.** 2010. National select agent registry. U.S. Department of Agriculture, Washington, DC. http://www.selectagents.gov.
35. **Chosewood LC.** 2009. Biosafety in microbiological and biomedical laboratories. U.S. Department of Health and Human Services, Washington, DC. http://www.cdc.gov/biosafety/publications/bmbl5/BMBL.pdf.
36. **U. S. Department of Agriculture.** 2011. Agricultural select agent. U.S. Department of Agriculture, Washington, DC. http://www.aphis.usda.gov/programs/ag_selectagent.
37. **Maines TR, Belser JA, Gustin KM, van Hoeven N, Zeng H, Svitek N, von Messling V, Katz JM, Tumpey TM.** 2012. Local innate immune responses and influenza virus transmission and virulence in ferrets. J. Infect. Dis. **205**:474–485.
38. **Mariassy AT.** 1991. Epithelial cells of trachea and bronchi, p 63–76. *In* Parent RA (ed), Comprehensive treatise on pulmonary toxicology: comparative biology of the normal lung. CRC Press, Inc, Boca Raton, FL.
39. **O'Donnell CD, Subbarao K.** 2011. The contribution of animal models to the understanding of the host range and virulence of influenza A viruses. Microbes Infect. **13**:502–515.
40. **Korteweg C, Gu J.** 2008. Pathology, molecular biology, and pathogenesis of avian influenza A (H5N1) infection in humans. Am. J. Pathol. **172**:1155–1170.
41. **Peiris JS, Yu WC, Leung CW, Cheung CY, Ng WF, Nicholls JM, Ng TK, Chan KH, Lai ST, Lim WL, Yuen KY, Guan Y.** 2004. Re-emergence of fatal human influenza A subtype H5N1 disease. Lancet **363**:617–619.
42. **Piazza FM, Carson JL, Hu SC, Leigh MW.** 1991. Attachment of influenza A virus to ferret tracheal epithelium at different maturational stages. Am. J. Respir. Cell Mol. Biol. **4**:82–87.
43. **Srinivasan A, Viswanathan K, Raman R, Chandrasekaran A, Raguram S, Tumpey TM, Sasisekharan V, Sasisekharan R.** 2008. Quantitative biochemical rationale for differences in transmissibility of 1918 pandemic influenza A viruses. Proc. Natl. Acad. Sci. U. S. A. **105**:2800–2805.
44. **Harkema JR, George MA, Hyde DM, Plopper CG.** 1991. Epithelial cells of the conducting airways, p 3–39. *In* Farmer SG, Hay DW (ed), The airway epithelium: physiology, pathophysiology, and pharmacology, **vol 55**. Marcel Dekker, Inc, New York, NY.
45. **Hoke CH, Jr, Hopkins JA, Meiklejohn G, Mostow SR.** 1979. Comparison of several wild-type influenza viruses in the ferret tracheal organ culture system. Rev. Infect. Dis. **1**:946–954.
46. **Hill DB, Button B.** 2012. Establishment of respiratory air-liquid interface cultures and their use in studying mucin production, secretion, and function. Methods Mol. Biol. **842**:245–258.
47. **Gustin KM, Belser JA, Wadford DA, Pearce MB, Katz JM, Tumpey TM, Maines TR.** 2011. Influenza virus aerosol exposure and analytical system for ferrets. Proc. Natl. Acad. Sci. U. S. A. **108**:8432–8437.
48. **Zeng H, Pappas C, Belser JA, Houser KV, Zhong W, Wadford DA, Stevens T, Balczon R, Katz JM, Tumpey TM.** 2012. Human pulmonary microvascular endothelial cells support productive replication of highly pathogenic avian influenza viruses: possible involvement in the pathogenesis of human H5N1 virus infection. J. Virol. **86**:667–678.
49. **Cameron CM, Cameron MJ, Bermejo-Martin JF, Ran L, Xu L, Turner PV, Ran R, Danesh A, Fang Y, Chan PK, Mytle N, Sullivan TJ, Collins TL, Johnson MG, Medina JC, Rowe T, Kelvin DJ.** 2008. Gene expression analysis of host innate immune responses during Lethal H5N1 infection in ferrets. J. Virol. **82**:11308–11317.
50. **Svitek N, Rudd PA, Obojes K, Pillet S, von Messling V.** 2008. Severe seasonal influenza in ferrets correlates with reduced interferon and increased IL-6 induction. Virology **376**:53–59.
51. **McFadden ER, Jr, Pichurko BM, Bowman HF, Ingenito E, Burns S, Dowling N, Solway J.** 1985. Thermal mapping of the airways in humans. J. Appl. Physiol. **58**:564–570.
52. **Massin P, van der Werf S, Naffakh N.** 2001. Residue 627 of PB2 is a determinant of cold sensitivity in RNA replication of avian influenza viruses. J. Virol. **75**:5398–5404.
53. **Maines TR, Chen LM, Matsuoka Y, Chen H, Rowe T, Ortin J, Falcon A, Nguyen TH, Mai Le Q, Sedyaningsih ER, Harun S, Tumpey TM, Donis RO, Cox NJ, Subbarao K, Katz JM.** 2006. Lack of transmission of H5N1 avian-human reassortant influenza viruses in a ferret model. Proc. Natl. Acad. Sci. U. S. A. **103**:12121–12126.
54. **Uyeki TM.** 2009. Human infection with highly pathogenic avian influenza A (H5N1) virus: review of clinical issues. Clin. Infect. Dis. **49**:279–290.